Published in final edited form as:
Science. 2010 January 8; 327(5962): 213. doi:10.1126/science.1179438.

Essential Role of the Histone Methyltransferase G9a in Cocaine-induced Plasticity

Ian Maze[1], **Herbert E. Covington III**[1], **David M. Dietz**[1], **Quincey LaPlant**[1,2], **William Renthal**[2], **Scott J. Russo**[1], **Max Mechanic**[2], **Ezekiell Mouzon**[1], **Rachael L. Neve**[3], **Stephen J. Haggarty**[4,5], **Yanhua Ren**[1], **Srihari C. Sampath**[6], **Yasmin L. Hurd**[1], **Paul Greengard**[7], **Alexander Tarakhovsky**[6], **Anne Schaefer**[7], and **Eric J. Nestler**[1,*]

[1] Fishberg Department of Neuroscience, Mount Sinai School of Medicine, New York, NY

[2] Departments of Psychiatry and Neuroscience, The University of Texas Southwestern Medical Center, Dallas, TX

[3] Department of Brain and Cognitive Sciences, Massachusetts Institute of Technology, Cambridge, MA

[4] Psychiatric and Neurodevelopmental Genetics Unit and Molecular Neurogenetics Unit, Center for Human Genetic Research, Massachusetts General Hospital, Boston, MA

[5] Stanley Center for Psychiatric Research, Broad Institute of Harvard and Massachusetts Institute of Technology, Cambridge, MA

[6] Laboratory of Lymphocyte Signaling, The Rockefeller University, New York, NY

[7] Laboratory of Molecular and Cellular Neuroscience, The Rockefeller University, New York, NY

Abstract

Cocaine-induced alterations in gene expression cause changes in neuronal morphology and behavior that may underlie cocaine addiction. We identified an essential role for histone 3 lysine 9 (H3K9) dimethylation and the lysine dimethyltransferase G9a in cocaine-induced structural and behavioral plasticity. Repeated cocaine administration reduced global levels of H3K9 dimethylation in the nucleus accumbens. This reduction in histone methylation was mediated through the repression of G9a in this brain region, which was regulated by the cocaine-induced transcription factor ΔFosB. Using conditional mutagenesis and viral-mediated gene transfer, we found that G9a downregulation increased dendritic spine plasticity of nucleus accumbens neurons and enhanced preference for cocaine, thereby establishing a crucial role for histone methylation in the long-term actions of cocaine.

Repeated cocaine exposure is characterized by persistent changes in gene expression and altered neuronal morphology within the nucleus accumbens (NAc), a key component of the brain's reward circuitry (1–2). Chromatin remodeling is important in aberrant transcriptional changes in this brain region that may underlie aspects of cocaine addiction (3–9). Cocaine regulation of chromatin structure in the NAc results, in part, from direct cocaine-induced modifications of the chromatin enzymatic machinery, leading to changes in histone acetylation

*To whom correspondence should be addressed. eric.nestler@mssm.edu.

I certify that none of the materials included within the manuscript entitled *Essential Role of the Histone Methyltransferase G9a in Cocaine-induced Plasticity* have been previously published or are under consideration elsewhere, including on the Internet.

All work involving the use of animals was conducted in accordance with institutional and IACUC guidelines at both The University of Texas Southwestern Medical Center and Mount Sinai School of Medicine.

and phosphorylation (4,7–9); however, roles for enzymes controlling histone methylation have not yet been investigated.

A recent genome-wide promoter analysis using chromatin immunoprecipitation coupled to microarrays (ChIP-Chip) identified altered patterns of repressive histone H3 lysine 9 (H3K9) and 27 (H3K27) methylation at specific gene promoters in the NAc following repeated cocaine treatment (6). We therefore profiled numerous lysine methyltransferases (KMTs) and demethylases (KDMs) that are known to control H3K9 or H3K27 methylation (Fig. 1A). Only two enzymes, G9a and GLP, displayed persistent transcriptional regulation 24 hours after repeated cocaine administration, when the expression of both genes was significantly downregulated. Because G9a and GLP specifically catalyze the dimethylation of H3K9 (H3K9me2), their downregulation by cocaine is consistent with decreased global levels of euchromatic H3K9me2 observed at this time point (Fig. 1B). In contrast, global levels of heterochromatic H3K27 methylation remained unaltered by repeated cocaine exposure (Fig. S1 in supporting online material). Due to its high levels of catalytic activity both *in vitro* and *in vivo* (10), we set out to further investigate the functional significance of G9a repression following repeated cocaine exposure in the NAc. Levels of G9a protein, like levels of its mRNA, were significantly reduced 24 hours after repeated cocaine administration (Fig. S2). Although G9a mRNA expression was reduced by 35% in the NAc, immunohistochemical analysis revealed a more modest 15% reduction in G9a protein levels, consistent with the observed 21% decrease in H3K9me2 after repeated cocaine administration (Fig. 1B). G9a mRNA expression was also downregulated in this brain region by 20% following repeated self-administration of cocaine (Fig. S3).

To identify whether changes in euchromatic H3K9me2 correlate with genome-wide alterations in gene expression in the NAc, we employed microarray analyses to examine gene expression profiles induced by a challenge dose of cocaine in animals with or without a history of prior cocaine exposure (see supplemental gene lists in Tables S1–S3). Animals that had received repeated cocaine displayed dramatically increased gene expression 1 hour after a cocaine challenge in comparison to acutely treated animals (Fig. 1C). This increased gene expression still occurred in response to a cocaine challenge given after 1 week of withdrawal from repeated cocaine. Consistent with previous reports, a small percentage of genes (~10%) displayed desensitized transcriptional responses following repeated cocaine administration (Fig. 1C; see Table S1) (5). To directly investigate the role of G9a downregulation in the enhanced gene expression observed after repeated cocaine, mice received intra-NAc injections of Herpes simplex virus (HSV) vectors expressing either GFP or G9a and were treated with saline or repeated cocaine to determine whether G9a overexpression was sufficient to block the repeated cocaine-induced enhancement of gene expression. From a set of 12 randomly selected genes displaying heightened levels of expression following repeated cocaine, we observed that G9a significantly reduced the enhanced expression of 50% of these genes (Table S4).

To identify upstream transcriptional events that mediate the repeated cocaine-induced repression of G9a expression, we investigated a possible role for ΔFosB, a highly stable splice product of the immediate early gene *fosB*. ΔFosB accumulates in the NAc after repeated exposure to cocaine, where it has been linked to increased cocaine reward (11). ΔFosB can act as either a transcriptional activator or repressor depending on the target gene involved (3,5,6, 12). Using bitransgenic NSE-*tTA* × tetOP-Δ*FosB* mice, wherein ΔFosB expression can be induced selectively in the NAc and dorsal striatum of adult animals (13), we examined the impact of ΔFosB expression on cocaine regulation of H3K9me2 and KMTs in the NAc. ΔFosB overexpression was sufficient to reduce levels of both H3K9me2 (Fig. 1D) and G9a expression (Fig. 1E), thereby mimicking the effects of repeated cocaine. In contrast, ΔFosB did not reduce GLP expression in this brain region, and had no effect on SUV39H1 and EZH2, the principal trimethylating enzymes for H3K9 and H3K27, respectively (Fig. S4). To confirm these data

using an independent ΔFosB overexpression system, wildtype adult mice received bilateral intra-NAc injections of Adeno-associated virus (AAV) vectors expressing either GFP or ΔFosB. Viral-mediated overexpression of ΔFosB decreased levels of G9a expression in this brain region (Fig. 1E).

Such pronounced and specific regulation of G9a prompted us to investigate whether altering G9a expression specifically in NAc neurons regulates behavioral responses to cocaine. Wildtype mice received intra-NAc injections of HSV vectors expressing GFP or G9a and were then analyzed using an unbiased cocaine conditioned place preference paradigm, which provides an indirect measure of drug reward. Viral overexpression of G9a in NAc neurons was confirmed following behavioral testing (Fig. 2A). G9a overexpression significantly decreased preference for cocaine in comparison to animals overexpressing GFP (Fig. 2B), and increased H3K9me2 levels in the NAc (Fig. 2C). Overexpression of a catalytically dead mutant of G9a (G9aH1093K) (14) did not affect cocaine preference (Fig. 2B) and had no affect on H3K9me2 levels in this brain region (Fig. 2C).

To further study the role of G9a in the behavioral effects of cocaine, and more specifically to mimic the repeated cocaine-induced repression of G9a expression in the NAc, adult $G9a^{fl/fl}$ mice (14) received intra-NAc injections of AAV vectors expressing Cre recombinase or GFP as a control. AAV-Cre knockdown of G9a in the NAc, which was confirmed immunohistochemically (Fig. S5), significantly increased the effects of cocaine in place conditioning experiments and decreased H3K9me2 levels in the NAc (Fig. 2D, E). A commercially available pharmacological inhibitor of G9a and GLP, BIX01294 (15–16), was used to ascertain whether enzyme inhibition similarly affects behavioral responses to cocaine. Indeed, pharmacological inhibition of G9a and GLP significantly increased preference for cocaine and decreased H3K9me2 in the NAc (Fig. 2F, G).

Repeated administration of cocaine increases the density of dendritic spines on NAc medium spiny neurons (17), a process associated with functional changes at excitatory glutamatergic synapses onto these neurons (18–19) and sensitized behavioral responses to the drug (17,20). We thus hypothesized that downregulation of G9a activity in the NAc by repeated cocaine might mediate cocaine's ability to regulate the dendritic spine density of NAc neurons. Using chromatin immunoprecipitation (ChIP) with an anti-G9a antibody, we identified several putative G9a gene targets in the NAc, each of which has previously been implicated in cocaine-induced dendritic plasticity (Fig. 3A) (20–26). We found that repeated cocaine administration significantly decreased G9a binding, as well as levels of H3K9me2, at these gene promoters (Fig. 3B). In contrast, acute cocaine administration rapidly recruited G9a to some of these same gene promoters, consistent with increased G9a expression observed in the NAc 1 hour after an acute dose of cocaine (Fig. S6). Although G9a binding at specific gene promoters correlates with changes in its expression, it remains unclear as to whether such events are mediated by altered global levels of G9a in the NAc and/or by differences in G9a recruitment following acute *v.s.* repeated cocaine administration.

Based on G9a's regulation of numerous plasticity-related genes in the NAc, we examined directly whether maintenance of G9a expression in this brain region following repeated cocaine treatment was sufficient to block cocaine-induced dendritic spine formation. Using a cocaine treatment protocol previously demonstrated to promote dendritic spine induction in the NAc (20), we examined spine density in animals injected with either HSV-GFP or HSV-G9a. In agreement with previous findings, we observed a significant increase in dendritic spine density in the NAc following cocaine treatment, an effect that was blocked completely by G9a overexpression (Fig. 3C). G9a overexpression alone was not sufficient to decrease NAc dendritic spine density in the absence of cocaine. To complement these data, $G9a^{fl/fl}$ mice received intra-NAc injections of HSV-Cre and spine density was quantified and compared to

animals receiving HSV-GFP in the absence of cocaine. Knockdown of G9a expression significantly increased spine density on NAc medium spiny neurons (Fig. 3C).

Given the evidence that G9a downregulation in the NAc after repeated cocaine is mediated by ΔFosB, we next examined whether this transcription factor is likewise involved in the regulation of NAc dendritic spines. Although ΔFosB has not previously been linked causally to such dendritic plasticity, several of its targets, including Cdk5 and NFκB subunits, have been so implicated (20–23), and ΔFosB's persistent expression in NAc neurons correlates with increased dendritic spine density after repeated cocaine treatment (27). First, we found that induction of ΔFosB in bitransgenic mice in the absence of cocaine, which downregulated G9a and H3K9me2 expression (Fig. 1D, E), decreased G9a binding to numerous plasticity-related genes, many of which have also been shown to be direct targets of ΔFosB itself (Fig. 3D) (3, 6). We next showed that viral overexpression of ΔFosB in the NAc significantly increased dendritic spine density under basal conditions, similar to that observed following repeated cocaine administration (Fig. 3E). Conversely, overexpression in the NAc of ΔJunD, a dominant negative mutant protein that antagonizes ΔFosB transcriptional activity, blocked the ability of repeated cocaine to increase dendritic spine formation in the NAc (Fig. 3C).

Our observation that ΔFosB regulates G9a expression in the NAc, and that ΔFosB and G9a regulate some of the same target genes, led us to examine other interactions between ΔFosB and G9a. After acute cocaine, when G9a levels were increased, binding of G9a to the *fosB* gene was increased, while after repeated cocaine, when G9a expression was suppressed, G9a binding to the *fosB* gene was decreased (Fig. 3A). Such decreased G9a binding after repeated cocaine was not observed for *c-fos,* where G9a binding is increased by repeated cocaine (Fig. S7). This is consistent with the fact that, unlike *fosB*, *c-fos* is repressed, not induced, by chronic psychostimulant exposure (5). ΔFosB overexpression in bitransgenic mice was sufficient to significantly decrease G9a binding to the *fosb* gene (Fig. 3D). Furthermore, G9a overexpression was sufficient to reduce increased ΔFosB expression following repeated cocaine administration (Table S4). These data suggest an autoregulatory loop whereby G9a initially limits induction of ΔFosB by acute cocaine administration. However, as ΔFosB accumulates with repeated drug exposure, it represses G9a and thereby potentiates its own further induction.

In conclusion, we have demonstrated that histone lysine methylation in the NAc is critically involved in regulating neuronal gene expression in response to cocaine. Repression of G9a and H3K9me2 following repeated cocaine administration promotes cocaine preference, in part, through the transcriptional activation of numerous genes known to regulate aberrant forms of dendritic plasticity. Gaining a better understanding of the genes being regulated through such mechanisms will improve our knowledge of the complex biological basis of drug addiction and could aid in the development of more effective treatments of addictive disorders.

Materials and Methods

Animals and treatments

Unless otherwise stated, mice were housed four to five per cage in a colony with a 12 hour light/dark cycle (lights on from 7:00 A.M. to 7:00 P.M.) at constant temperature (23°C) with *ad libitum* access to water and food. All animal protocols were approved by IACUC at both UT Southwestern Medical Center and Mount Sinai School of Medicine.

For cocaine experiments [immunohistochemitry, western blotting, quantitative PCR (qPCR), microarray analysis and chromatin immunoprecipitation (ChIP)], 8- to 10-week-old male C57BL/6J mice were used. Animals received daily injections of either 'saline' (7 treatments saline, i.p.), 'acute' cocaine (6 treatments saline + one treatment 20 mg/kg cocaine-HCl, i.p.)

or 'repeated' cocaine (7 treatments 20 mg/kg cocaine-HCl, i.p.). Mice were sacrificed at either 1 hour or 24 hours following the final treatment. For microarray studies, animals were treated daily with either 'saline' (15 treatments saline, i.p.), 'acute' cocaine (14 treatments saline + 1 treatment 20 mg/kg cocaine-HCl, i.p.), 'repeated + acute' cocaine (7 treatments saline + 8 treatments 20 mg/kg cocaine-HCl, i.p.) or 'repeated withdrawal + acute' cocaine (7 treatments 20 mg/kg cocaine-HCl + 7 treatments saline + 1 challenge treatment 20 mg/kg cocaine-HCl, i.p.) and were sacrificed 1 hour after the final treatment. In behavioral experiments, mice were singly housed post-surgery and were treated with 10 mg/kg cocaine-HCl, i.p. as described below. For dendritic spine analysis and microarray validation following HSV-GFP and HSV-G9a-GFP infection, mice were treated with 'saline' (5 treatments saline, i.p.) or 'repeated cocaine' (5 treatments 20 mg/kg cocaine-HCl, i.p.) over the course of 3 days, as this injection protocol has previously been demonstrated to increase spine density on nucleus accumbens (NAc) neurons within the timeframe of Herpes simplex virus (HSV) transgene expression (Supplemental ref S1). Mice used for dendritic spine analysis were sacrificed 4 hours following the last treatment.

To induce local deletion of the G9a transcript restricted to NAc neurons, we used mutant mice homozygous for a floxed G9a allele, which have been described in detail elsewhere (*S2*). Cre-induced recombination produces exon 22 to 25 out-of-frame splicing leading to nonsense-mediated decay of the mutated transcript. We used G9a floxed mice that were fully backcrossed to C57BL/6J mice. Mice were sterotaxically-injected into the NAc with Adeno-associated virus (AAV) vectors (serotype 2) expressing GFP or Cre-GFP between the age of 7 and 10 weeks. Immunohistochemical analysis was used to verify the efficiency of Cre-mediated recombination (see Supplemental Fig. S5). We used AAV injected animals 21 days post-surgery because recombination in G9a floxed mice was stable and maximal at this time-point, consistent with published reports (*S3–S4*). G9a and ΔJunD overexpression experiments were similarly conducted using HSV virus vectors expressing either GFP, wildtype G9a-GFP, catalytically dead G9aH1093K-GFP or ΔJunD-GFP (see *S2* for details concerning the development of G9a constructs). HSV overexpressing mice were used 3 days post-surgery since overexpression was maximal at this time-point, as observed via immunohistochemistry. Due to the transient nature of HSV expression, and the considerably more stable nature of AAV expression, HSV vectors were used in experiments requiring fast, short-term transgene expression, whereas AAV vectors were used in experiments requiring extended periods of transgene expression. Both vectors have been shown, in extensive prior studies, to infect only neuronal cell bodies within the injected brain area, without any infection of afferent or efferent neurons.

For behavioral experiments using the pharmacological G9a/GLP inhibitor, BIX01294 (25 ng/μl), mice were sterotaxically implanted with two subcutaneous mini-pumps, as well as bilateral guide cannulae, into the NAc. Mini-pumps were activated 12 hours prior to implantation initiating the continuous delivery (0.25 μl/hour) of either vehicle (5 hydroxypropyl β-cyclodextrin) or drug for 14 days, during which time behavioral evaluations were performed.

For ΔFosB overexpression experiments [western blotting, qPCR, and ChIP], male bitransgenic NSE-*tTA* × tetOP-Δ*FosB* mice were used (10 week-old), whereby in the absence of the tetracycline derivative doxycycline (8 weeks off doxycycline), animals displayed robust striatal restricted constitutive expression of ΔFosB (*S5*). ΔFosB overexpression in these mice was confirmed via qPCR. To confirm findings using NSE-*tTA* × tetOP-Δ*FosB* mice, wildtype 8-week-old C57BL/6J male mice were sterotaxically-injected intra-NAc with AAV vectors expressing either GFP or ΔFosB-GFP. AAV vectors were used, in this case, to ensure maximal ΔFosB expression at 8 weeks post-surgery, allowing for a direct comparison between virally infected and bitransgenic ΔFosB overexpressing mice. Viral overexpression was confirmed using qPCR at 8 weeks post-surgery (15-gauge NAc punches were dissected under the injection

site). AAV-GFP and AAV-ΔFosB-GFP overexpressing mice that were not used for qPCR were treated with saline (14 treatments saline, i.p.) or repeated cocaine (14 treatments 30 mg/kg cocaine-HCl, i.p.) beginning at 6 weeks post-surgery. 4 days following the final treatment, brains were fixed with 4% paraformaldehyde, sectioned on a vibratome and used for dendritic spine analysis.

Western blot analysis

14-gauge NAc punches were taken from 1 mm coronal sections obtained using a stainless steel mouse brain matrix and were sonicated in 1 M HEPES lysis buffer (1% SDS) containing protease and phosphatase inhibitors. 10–30 μg samples of total protein were electrophoresed on 18% SDS gels. Proteins were transferred to PVDF membranes and incubated with either anti-H3K9me2 (mouse monoclonal, 1:500), anti-β-tubulin (mouse monoclonal, 1:60,000), anti-total histone H3 (rabbit polyclonal, 1:5,000), anti-GFP (used for verification of equal viral expression in punched tissue) (rabbit polyclonal, 1:1000), anti-H3K27me3 (rabbit polyclonal, 1:500) or anti-actin antibodies (mouse monoclonal, 1:60,000) overnight at 4°C (all membranes were blocked in 5% milk or 5% bovine serum albumin). Membranes were then incubated with peroxidase-labeled secondary antibodies (1:15,000–1:60,000 depending on the primary antibody used) and bands were visualized using SuperSignal West Dura substrate. Bands were quantified with NIH Image J Software and H3K9me2 bands were normalized to either actin or β-tubulin and to total histone H3 to control for equal loading. Repeated cocaine had no effect on levels of actin (Fig. S8) or total histone 3 (Fig. S1) in the NAc. Furthermore, HSV-G9a-GFP and HSV-G9aH1093K-GFP infection had no effect on total levels of β-tubulin in the NAc (Fig. S8).

Immunohistochemistry

Mice were sedated with a lethal dose of chloral hydrate and perfused with 4% paraformaldehyde before being analyzed by single or double immunohistochemistry as previously described (*S6*). Briefly, post-fixed brains were incubated at room temperature overnight in 30% sucrose before being sectioned at 35 μm (brains used for dendritic spine analysis were sectioned on a vibratome at 100 μm sections in the absence of 30% sucrose). Free-floating NAc sections were washed with 1X PBS, blocked (3% normal donkey serum, 0.1% tritonX, 1X PBS) and later incubated with anti-GFP (chicken polyclonal, 1:8000) and/or anti-G9a (rabbit polyclonal, 1:500) antibodies in blocking solution. Sections analyzed for dendritic spines were incubated with a rabbit polyclonal anti-GFP antibody at 1:200. Following overnight incubation, NAc sections were rinsed 3 times for 10 minutes with 1X PBS, followed by incubation with Cy2 and/or Cy3 fluorescent-coupled secondary antibodies in 1X PBS blocking solution for 2 hours. Sections used for morphology studies were incubated in secondary antibody overnight at room temperature. Nuclear co-staining was achieved by incubating sections in 1X PBS containing DAPI (1:50,000) for 10 minutes. Sections were once again washed, followed by ethanol dehydration and mounting with DPX. All sections were imaged using confocal microscopy.

RNA isolation and qPCR

Bilateral 14-gauge NAc punches were homogenized in Trizol and processed according to the manufacturer's instructions. RNA was purified with RNAesy Micro columns and spectroscopy confirmed that the RNA 260/280 and 260/230 rations were >1.8. RNA was then reverse transcribed using a Bio-Rad iScript Kit. cDNA was quantified by qPCR using SYBR Green. Each reaction was run in duplicate or triplicate and analyzed following the ΔΔCt method as previously described using glyceraldehyde-3-phosphate dehydrogenase (GAPDH) as a normalization control (*S7*). See supplemental Table S5 for mRNA primer sequences.

DNA microarray analysis

Four groups (3 independent biological replicates per group) were utilized for the microarray study, totaling 12 microarrays. 1 hour following the last cocaine injection, animals were rapidly decapitated and brains were removed and placed on ice. Dissections of NAc were taken using a 15-gauge needle punch and were quickly frozen on dry ice until RNA was extracted. Bilateral punches were pooled from four animals per replicate, totaling 12 mice per group. RNA isolation, microarray processing, and data analysis were performed as previously described (*S8*). Briefly, RNA was isolated and purified as described above and was checked for quality using Agilent's Bioanalyzer. Reverse transcription, amplification, labeling and hybridization to Illumina MouseWG-6 v2.0 arrays were performed using standard procedures by UT Southwestern's microarray core. Raw data were background subtracted and quantile normalized using Beadstudio software. Normalized data were analyzed using GeneSpring software and genelists were generated using significance criteria of a 1.3 fold change cutoff coupled with a non-stringent p-value cutoff of $p < 0.05$.

We maintain a high degree of confidence in these data for several reasons. First, all animals were handled, treated and killed at the same time, under the same conditions. As well, all RNA and array processing was performed at the same time. Second, we performed triplicate arrays and pooled multiple animals per array sample, thereby minimizing differences due to individual variability and increasing statistical power (*S9*). Third, the data analysis criteria used for our study are recommended by the MicroArray Quality Control project, as these criteria have been validated to provide a high degree of intersite reproducibility and inter- and intraplatform reproducibility (*S10–S11*).

Construction of viral vectors

Due to viral vector insertion size constraints, coding sequences for either wildtype G9a (G9a) or catalytically dead G9a (G9aH1093K) were subcloned into the bicistronic p1005+ HSV plasmid expressing GFP under the control of the human immediate early cytomegalovirus promoter (CMV) (the G9a insertion size was ~ 3.96 kb, which exceeds the maximum insertion size for AAV-2 vectors). The IE4/5 promoter drives G9a expression. Fragments were subcloned into the bicistronic p1005+ HSV plasmid via blunt end ligations with Klenow treated PmeI and EcoRI digested G9a (from pcDNA3.1) and CIP treated p1005+ following EcoRI digestion. For production of HSV-ΔJunD-GFP, the coding sequence of ΔJunD flanked by EcoRI restriction sites was generated by PCR using primer oligonucleotides containing the EcoRI site. The PCR product was then ligated into the EcoRI site of the p1005+ vector. Local expression of Cre recombinase in NAc neurons was achieved by viral-mediated gene delivery using an AAV vector as described (*S12*). GFP or an N-terminal fusion of GFP to Cre was subcloned into a recombinant AAV-2 vector containing a CMV promoter with a splice donor acceptor sequence and polyadenylation signal. All vector insertions were confirmed by dideoxy-sequencing. Viral vectors were produced using a triple-transfection, helper-free method, as previously described (*S13*). Purified virus was stored at −80°C. Viral quality was assessed by infectious titer evaluated in HEK293 cells. AAV-ΔFosB-GFP viruses were similarly prepared. For HSV-Cre, Cre expression was driven by an IRES promoter, as opposed to the IE4/5 promoter, in order to minimize Cre expression and prevent neuronal toxicity (see *S14* for viral construction). In all cases, viral overexpression was validated, both *in vitro* and *in vivo,* via qPCR, and viruses were immunohistochemically confirmed to display NAc-restricted expression following surgery.

Stereotaxic surgery

Under ketamine (100 mg/kg)/xylazine (10 mg/kg) anesthesia, mice were positioned in a small-animal stereotaxic instrument, and the cranial surface was exposed. Thirty-three gauge syringe needles were used to bilaterally infuse 0.5 μl of virus into the NAc at a 10° angle (AP + 1.6;

ML + 1.5; DV − 4.4) at a rate of 0.1 μl/min. Animals receiving HSV injections were allowed to recover for 2 days following surgery, while mice used for behavioral testing receiving AAV vectors were allowed to recover for 20 days before being subjected to place conditioning. These times are consistent with the periods of maximal viral-mediated transgene expression for the two vectors. For BIX01294 infusions, each of two mini-pumps were positioned subcutaneously on the mouse's back. Cannulae placements were achieved by drilling two small cranial holes above the NAc, and by the delivery of the cannula from bregma (AP + 1.5; ML + 1.0; DV − 5.4). Mice were allowed to recover from surgery for 4 to 5 days before beginning the place conditioning procedure to cocaine as described below.

Conditioned place preference

The place conditioning procedure was conducted as previously described, with the following modifications (*S7*). Briefly, 3 days after intra-NAc infusions of HSV-G9a-GFP, HSV-G9aH1093K-GFP or HSV-GFP, mice were placed into the conditioning chambers, which consist of three distinct environments. Mice that showed significant preference for either of the two conditioning chambers were excluded from the study (<10% of all animals). Conditioning groups were then balanced to adjust for any chamber bias that may still exist. On subsequent days, animals were injected with saline and confined to one chamber in the afternoon for 30 minutes and then injected with cocaine (10 mg/kg, i.p.) and confined for 30 minutes to the other chamber in the evening for 2 days (two saline and two cocaine pairings). On the day of the test, mice were placed back into the apparatus without treatment for 20 minutes and tested to evaluate which side they preferred. Locomotor responses to cocaine were assessed via beam breaks in the cocaine-paired chambers to ensure effectiveness of drug treatment. For AAV and BIX01294 CPP experiments, a slightly modified protocol was employed. Animals were again injected with either saline or cocaine (10 mg/kg, i.p.) and confined to specific chambers for 30 minute sessions, but instead were only conditioned once a day for 4 days, followed by the test on day 5 (animals were conditioned in the evening and conditioning treatments were alternated). For all groups, baseline locomotion in response to saline was assessed to ensure that locomotion was not affected by viral or inhibitor treatment.

Intravenous cocaine self-administration

Male adolescent Long-Evans rats, weighing 230–250 g at the beginning of the experiment, were obtained. They were housed in a humidity- and temperature-controlled environment on a reversed 12 hour light/dark cycle (lights off at 9:00 a.m.) with *ad libitum* access to food and water. Rats were allowed to acclimate in their new environment and were handled daily for 1 week before the start of the experiment. All procedures were conducted in accordance with the National Institute of Health's Guide for the Care and Use of Laboratory Animals and were approved by Mount Sinai's Animal Care and Use Committee. The self-administration equipment was fitted with infrared beams to measure locomotor behavior. Self-administration was carried out as previously described (*S15-S16*) with catheters implanted into the right jugular vein under isoflurane (2.4–2.7%) anesthesia. Catheters were flushed with 0.1 ml of a saline solution containing 10 U heparin and ampicillin (50 mg/kg). Following one week of recovery from surgery, self-administration training began during the dark phase of the light/dark cycle. Animals were allowed 3-hour daily access to cocaine (0.75 mg/kg/infusion) under a fixed ratio-1 (FR1) reinforcement schedule, where 1 active lever press resulted in a single infusion of drug. Rats stabilized their cocaine intake after 6 days (<15% variation in response rate over 3 consecutive days, with at least 75% responding on the reinforced lever). 24 hours after the final self-administration session, rats were quickly decapitated, brains rapidly removed and processed for RNA isolation and qPCR.

Chromatin immunoprecipitation (ChIP)

Fresh NAc punches were formaldehyde cross-linked and prepared for ChIP as previously described (*S17-S18*) with minor modifications. Briefly, 4 14-gauge NAc punches per animal (5 animals pooled per sample) were collected, cross-linked with 1% formaldehyde and quenched with 2 M glycine before freezing at −80°C. 1 day prior to sample sonication, sheep anti-rabbit/mouse (depending on precipitation antibody) IgG magnetic beads were prepared by incubating appropriate magnetic beads with either anti-G9a (rabbit polyclonal ChIP grade) or anti-H3K9me2 (mouse monoclonal ChIP grade) antibodies overnight at 4°C under constant rotation in block solution. Tissue sonication and chromatin shearing were carried out as previously described (*S17*). Following sonication, equal concentrations of chromatin were transferred to new tubes and ~5% of the final products were saved to serve as 'input' controls. After thorough washing and resuspension of the conjugated bead/antibody mixtures, equal volumes of antibody/bead mixtures (~7.5 μg antibody/sample) were added to each chromatin sample and incubated for ~16 hours under constant rotation at 4°C. Samples were further washed and reverse cross-linked at 65°C overnight before DNA purification using a PCR purification kit. Following DNA purification, samples were subjected to qPCR and were normalized to their appropriate 'input' controls as previously described (*S17*). Normal mouse IgG immunoprecipitations using a mouse polyclonal anti-IgG antibody were also carried out to control for appropriate enrichment of signal amplification. Adenine phosphoribosyltransferase (APRT) was used as a negative control for cocaine and ΔFosB overexpression experiments. See Supplemental Table S5 for promoter primer sequences.

Dendritic spine analysis

To study the role of G9a in the regulation of neuronal morphology in vivo, we used methods previously described with the following modifications (*S1*). Three days after injection of HSV-GFP, HSV-G9a-GFP, HSV-ΔJunD-GFP (all viruses were used in wildtype C57Bl/6J mice), or HSV-Cre-GFP (used in $G9a^{fl/fl}$ mice), when viral expression was maximal, mice were perfused, brains were cryoprotected and later sectioned at 100 μm on a vibratome. Sections were then immunostained using an antibody against GFP as described above (see Immunohistochemistry). To assess the effects of G9a overexpression and knockout on spine numbers, as well as the effect of ΔJunD overexpression, we measured the number of spines on approximately 1–2 neurites per neuron equaling at least 299 μm of secondary dendrites from GFP-expressing NAc medium spiny neurons (MSNs). Given that MSNs are morphologically distinct from other neuronal populations in the NAc, as well as previous reports indicating that HSV primarily infects DARPP-32 expressing neurons in this brain region (*S19*), we are confident that MSNs were exclusively assessed in these studies. For each animal, we examined ~6–8 neurons in 3–4 animals per group (7 groups), after which an average value was obtained for each animal for statistical analysis. Experiments designed to examine the effects of ΔFosB overexpression on NAc spine density were carried similarly to that described above, with the exception that AAV vectors were used to express GFP or ΔFosB-GFP for extended periods of time (8 weeks). All HSV images were captured using a confocal microscope with a 100X oil-immersion objective (AAV images were captured with a 63X oil-immersion objective). Images were acquired with the pinhole set at 1 arbitrary unit and a 1024 × 1024 frame size. Dendritic length was measured using NIH Image J software, and spine numbers were counted blind by the primary experimenter, as slides were coded prior to experimental scanning. The average number of spines per 10 μm of dendrite was calculated.

Statistical analysis

One- and two-way ANOVAs were performed to determine significance for conditioned place preference and dendritic spine analysis with greater than two groups. Student's t tests were used for other comparisons including qPCR, western blotting, dendritic spine analysis

comparing HSV-GFP to HSV-Cre in G9a$^{fl/fl}$ mice, microarray analyses (see above) and chromatin immunoprecipitation experiments. Planned student's t-tests were used following two-way ANOVA analysis of dendritic spine density after ΔFosB overexpression with confirmation of significant main effects of drug treatment and virus. All values included in the figure legends represent mean ± SEM (*$p \leq 0.05$; **$p < 0.001$). Detailed statistical analyses for Figs. 1–3 in the main text are given in: Detailed Figure Legends Including Statistics.

Supplementary Material

Refer to Web version on PubMed Central for supplementary material.

References and Notes

1. Robinson TE, Kolb B. Neuropharmacology 2004;47(Suppl 1):33. [PubMed: 15464124]
2. Hyman SE, Malenka RC, Nestler EJ. Annu Rev Neurosci 2006;29:565. [PubMed: 16776597]
3. Kumar A, et al. Neuron 2005;48:303. [PubMed: 16242410]
4. Renthal W, et al. Neuron 2007;56:517. [PubMed: 17988634]
5. Renthal W, et al. J Neurosci 2008;28:7344. [PubMed: 18632938]
6. Renthal W, et al. Neuron 2009;62:335. [PubMed: 19447090]
7. Stipanovich A, et al. Nature 2008;453:879. [PubMed: 18496528]
8. Borrelli E, Nestler EJ, Allis CD, Sassone-Corsi P. Neuron 2008;60:961. [PubMed: 19109904]
9. Brami-Cherrier K, Roze E, Girault JA, Betuing S, Caboche J. JNeurochem 2009;108:1323. [PubMed: 19183268]
10. Tachibana M, Sugimoto K, Fukushima T, Shinkai Y. J Biol Chem 2001;276:25309. [PubMed: 11316813]
11. Nestler EJ. Philos Trans R Soc London, B Biol Sci 2008;363:3245. [PubMed: 18640924]
12. McClung CA, Nestler EJ. Nat Neurosci 2003;6:1208. [PubMed: 14566342]
13. Kelz MB, et al. Nature 1999;401:272. [PubMed: 10499584]
14. Sampath SC, et al. Mol Cell 2007;27:596. [PubMed: 17707231]
15. Kubicek S, et al. Mol Cell 2007;25:473. [PubMed: 17289593]
16. Chang Y, et al. Nat Struct Mol Biol 2009;16:312. [PubMed: 19219047]
17. Robinson TE, Kolb B. J Neurosci 1997;17:8491. [PubMed: 9334421]
18. Ungless MA, Whistler JL, Malenka RC, Bonci A. Nature 2001;411:583. [PubMed: 11385572]
19. Thomas MJ, Malenka RC. Philos Trans R Soc Lond B Biol Sci 2003;358:815. [PubMed: 12740128]
20. Russo SJ, et al. J Neurosci 2009;29:3529. [PubMed: 19295158]
21. Bibb JA, et al. Nature 2001;410:376. [PubMed: 11268215]
22. Norrholm SD, et al. Neuroscience 2003;116:19. [PubMed: 12535933]
23. Pulipparacharuvil S, et al. Neuron 2008;59:621. [PubMed: 18760698]
24. Ujike H, Takaki M, Kodama M, Kuroda S. Ann N Y Acad Sci 2002;965:55. [PubMed: 12105085]
25. Toda S, et al. J Neurosci 2006;26:1579. [PubMed: 16452681]
26. Graham DL. Nat Neurosci 2007;10:1029. [PubMed: 17618281]
27. Lee KW, et al. Proc Natl Acad Sci U S A 2006;103:3399. [PubMed: 16492766]

28. This work was supported by grants from the National Institute on Drug Abuse: P01 DA08227 (EJN), R01 DA07359 (EJN), and P0110044 (PG).

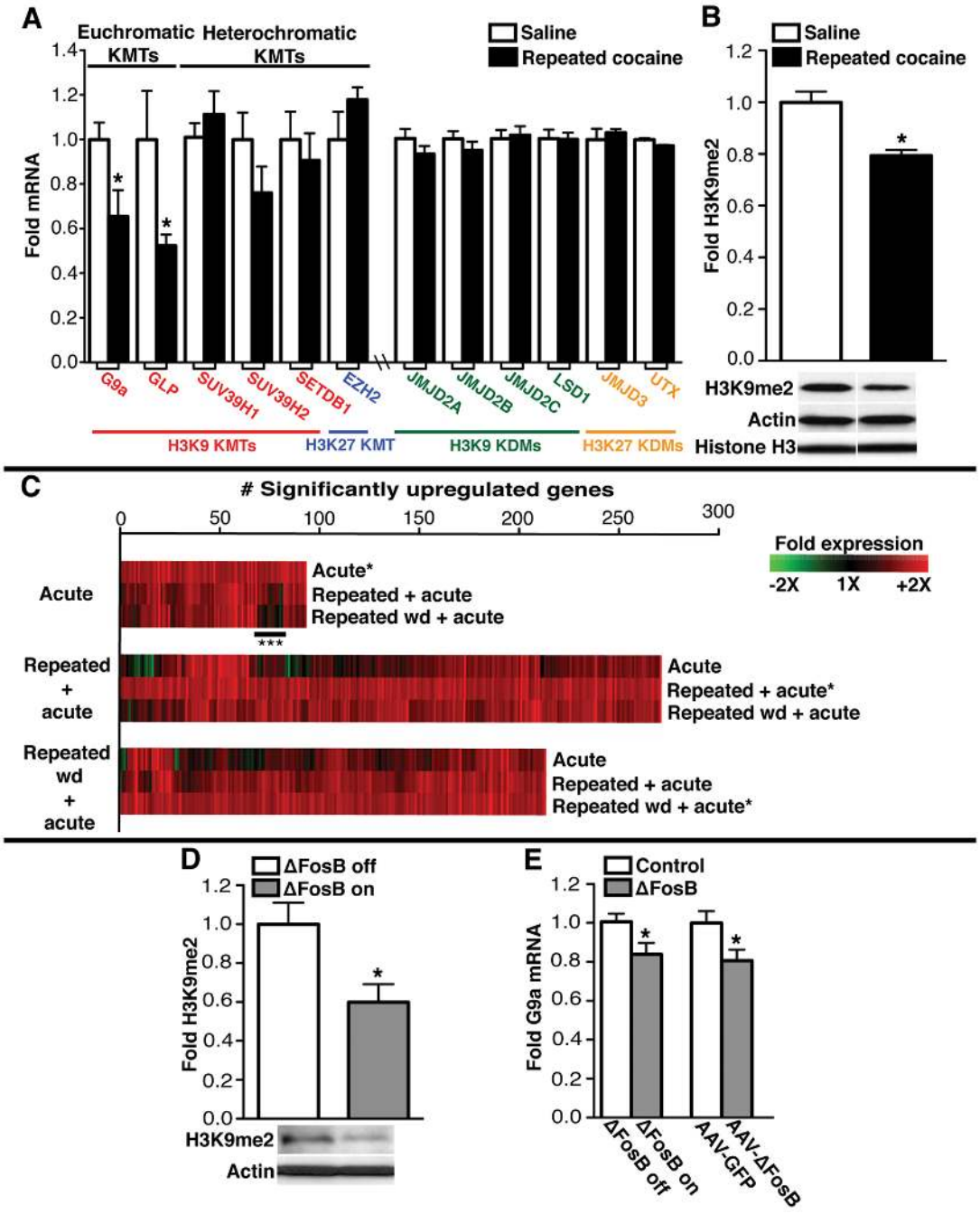

Fig. 1.

Repeated cocaine represses G9a expression in NAc through a ΔFosB-dependent mechanism. **(A)** mRNA expression of H3K9/K27 KMTs and KDMs in NAc 24 hr after repeated cocaine. **(B)** H3K9me2 levels in NAc 24 hr after repeated cocaine. **(C)** Analysis of gene expression after acute or repeated cocaine. Heatmaps (*) show genes upregulated in NAc 1 hr after a cocaine challenge in naïve animals (*Acute*), in animals treated repeatedly with cocaine (*Repeated + acute*) or in animals after 168 hr withdrawal from repeated cocaine (*Repeated wd + acute*). Associated heatmaps show how genes were affected under the other 2 conditions. Desensitized transcriptional responses following repeated cocaine are indicated (***). **(D)** H3K9me2 levels in NAc from NSE-*tTA* × tetOP-Δ*FosB* mice on ('Δ FosB off') or off ('Δ FosB

on') doxycycline 1 hr after repeated cocaine. **(E)** G9a mRNA expression in NAc from NSE-*tTA* × tetOP-Δ*FosB* mice on ('Δ FosB off') and off ('Δ FosB on') doxycycline, and from mice infected with AAV-GFP or AAV-ΔFosB. Data are presented as mean ± SEM. For statistical analyses, see full figure legends in "supporting online text."

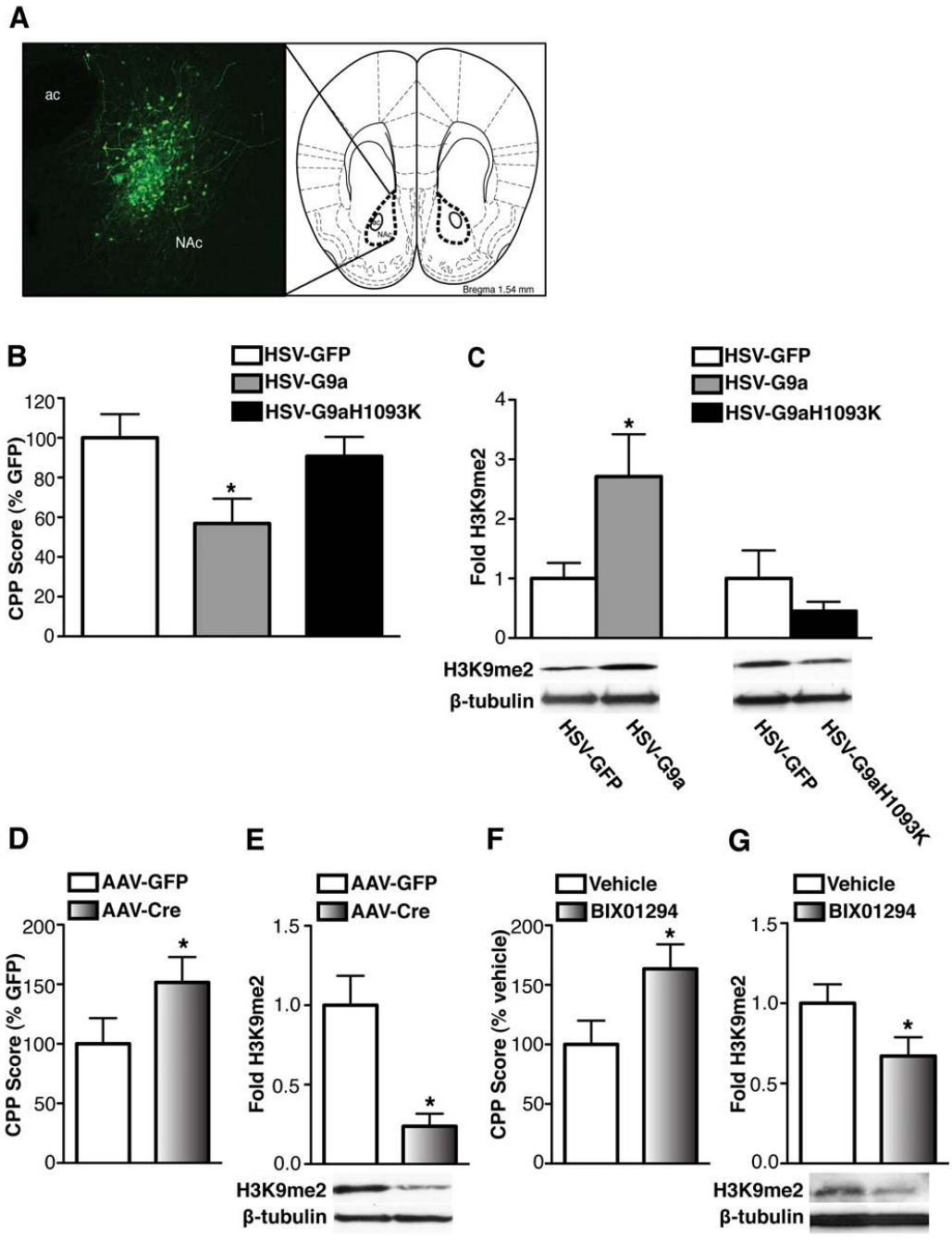

Fig. 2.

G9a in NAc regulates cocaine-induced behavioral plasticity. **(A)** Representative image of HSV-mediated transgene expression in NAc. Cartoon of the coronal brain slice was taken from the mouse brain atlas. **(B)** Conditioned place preference for cocaine and **(C)** H3K9me2 levels in NAc in animals infected with HSV-GFP, HSV-G9a, or HSV-G9aH1093K. **(D)** Conditioned place preference for cocaine and **(E)** H3K9me2 levels in NAc in $G9a^{fl/fl}$ animals infected with AAV-GFP or AAV-Cre. **(F)** Conditioned place preference for cocaine and **(G)** H3K9me2 levels in NAc in animals receiving intra-NAc vehicle or BIX01294. Data are presented as mean ± SEM.

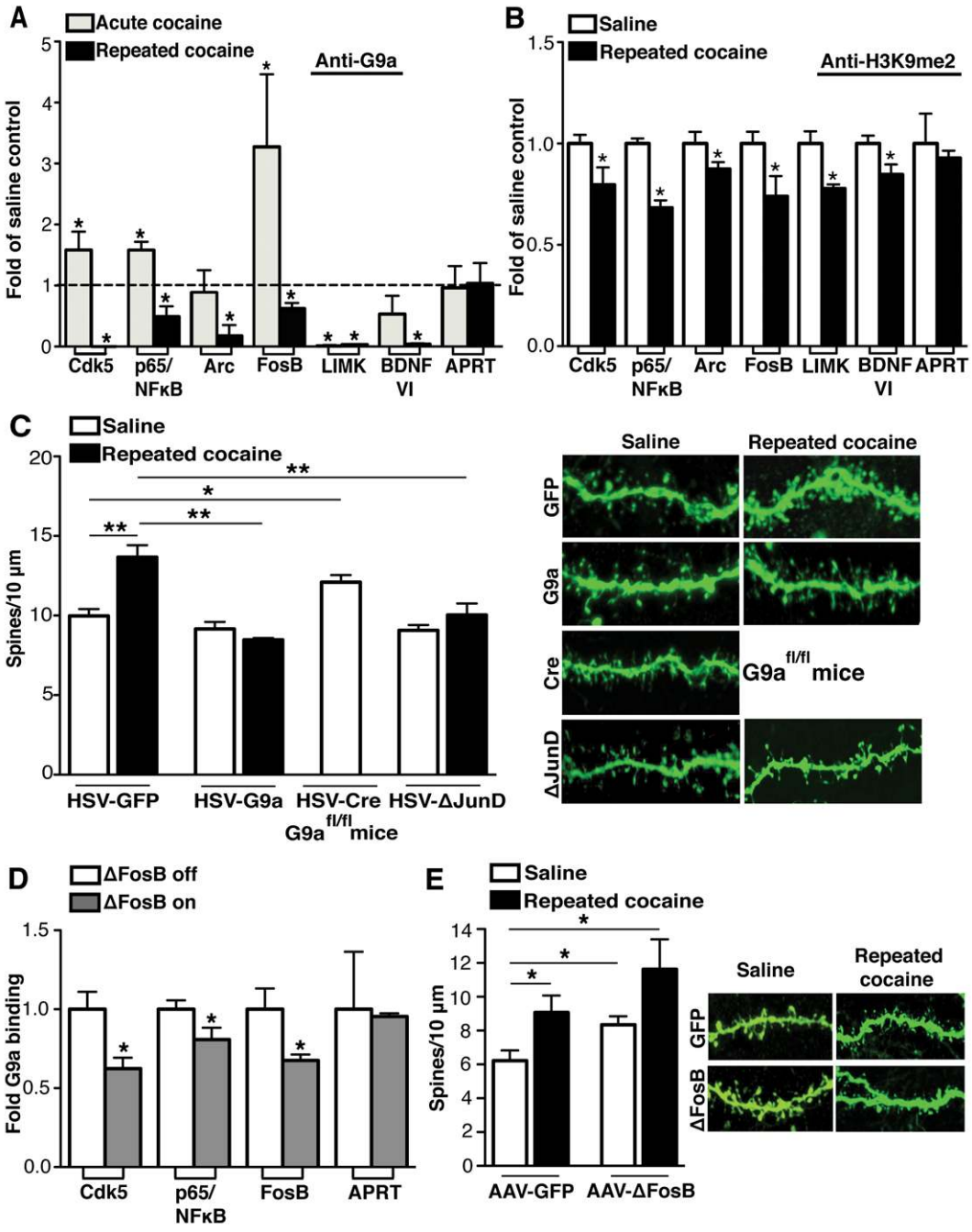

Fig. 3.

G9a in NAc regulates cocaine-induced dendritic spine plasticity. **(A)** Quantitative G9a ChIP in NAc from animals treated acutely or repeatedly with cocaine, at 1 or 24 hr, respectively. APRT was used as a negative control. Data are presented as the relative fold difference from saline controls. **(B)** Quantitative H3K9me2 ChIP in NAc from repeated cocaine-treated animals at 24 hr, presented as the relative fold difference from saline controls. **(C)** Dendritic spine analysis of animals infected with HSV-GFP, HSV-G9a, or HSV-ΔJunD following repeated cocaine, and dendritic spines in G9a$^{fl/fl}$ mice following HSV-Cre infection. **(D)** Quantitative G9a ChIP in NAc from NSE-*tTA* × tetOP-Δ*FosB* mice on ('ΔFosB off') and off ('Δ FosB on')

doxycycline. **(E)** Dendritic spine analysis in animals infected with AAV-GFP or AAV-ΔFosB following repeated cocaine. Data are presented as mean ± SEM.